

# A search for variable subdwarf B stars in *TESS* Full Frame Images III. An update on variable targets in both ecliptic hemispheres – contamination analysis and new sdB pulsators

S. K. Sahoo<sup>1,2\*</sup>, A. S. Baran<sup>2,3,4</sup>, H.L. Worters<sup>5</sup>, P. Németh<sup>2,6,7</sup> and D. Kilkenny<sup>8</sup>

<sup>1</sup>*Nicolaus Copernicus Astronomical Centre of the Polish Academy of Sciences, ul. Bartycka 18, 00-716 Warsaw, Poland*

<sup>2</sup>*ARDASTELLA Research Group*

<sup>3</sup>*Astronomical Observatory, University of Warsaw, Al. Ujazdowskie 4, 00-478 Warszawa, Poland*

<sup>4</sup>*Department of Physics, Astronomy, and Materials Science, Missouri State University, Springfield, MO 65897, USA*

<sup>5</sup>*South African Astronomical Observatory, Observatory 7935, South Africa*

<sup>6</sup>*Astronomical Institute of the Czech Academy of Sciences, Fričova 298, CZ-251 65 Ondřejov, Czech Republic*

<sup>7</sup>*Astroserver.org, Fő tér 1, 8533 Malomsok, Hungary*

<sup>8</sup>*Department of Physics and Astronomy, University of the Western Cape, Private Bag X17, Bellville 7535, South Africa*

Accepted XXX. Received YYY; in original form ZZZ

## ABSTRACT

We present an update on the variable star survey performed on the *TESS* 30 min Full Frame Image (FFI) data reported by our first two papers in this series. This update includes a contamination analysis in order to identify false positives and analysis of the *TESS* 10 min FFI data collected during Years 3 and 4 of the mission. We clarify the variability status of 2 995 targets identifying 1 403 variable stars. In addition, we spectroscopically classify 24 pre-filtered targets sampled with the 10 min FFI data and discover 11 new sdB pulsators. Future follow-up space- and/or ground-based data of variables reported here, to identify the nature of their variability and reveal spectroscopic parameters of the stars, would complement this work.

**Key words:** Stars: subdwarfs – Stars: oscillations (including pulsations) – asteroseismology

## 1 INTRODUCTION

Sahoo et al. (2020) (Paper I) and Baran et al. (2021) (Paper II) presented their results of variability checks of the most promising subdwarf B (sdB) candidates found in the Geier et al. (2019) and Geier (2020) catalogs. The former authors pre-selected 45 674 targets and used the Full Frame Images (FFI) collected by the *TESS* mission in the Southern Ecliptic Hemisphere (SEH) during Year 1 and in the Northern Ecliptic Hemisphere (NEH) during Year 2. As a result, 2 313 new variable targets in both ecliptic hemispheres were listed.

It is a well known feature of the *TESS* CCDs that an individual pixel has a 21 arcsec square projection on the sky. This makes contamination a serious problem. A contaminating star contributes by either increasing the average flux level in an aperture, thus lowering the apparent amplitude of flux variation in the target, or – if variable – makes a constant flux target star a false positive variable. The former issue can be corrected by removing the estimated amount of a contaminating star’s flux and this is fairly well achieved in the Pre-search Data Conditioning fluxes. The latter issue can only be resolved by checking the variability of all contaminants around

the target of interest. We also found this method useful to resolve variability in case both the target of interest and contaminator are variables.

In this work, we aimed to remove false positives from our list of 2 313 new variable objects. We searched all pixels within the target masks of all 2 313 objects listed in Papers I and II. In addition, for the most promising pulsating subdwarf candidates, we retrieved the new light curves from the FFI collected during Years 3 and 4, which are sampled at a 10 min cadence. This cadence extends the Nyquist frequency up to 833.3  $\mu$ Hz, which allows us to cover the entire gravity mode region in an amplitude spectrum<sup>1</sup>. By promising candidates, we mean objects that in Papers I and II show signals close to the Nyquist frequency of 277.7  $\mu$ Hz resulting from the 30 min cadence of observation used during Years 1 and 2.

To summarize the findings reported in Paper I and II, there are 15 pulsating subdwarf B star candidates, 79 variable (other than pulsating) sdB stars, 33 variable subdwarf candidates and 2 186 other variable stars, including 123 stars with non-sd classification.

<sup>1</sup> In hot subdwarfs, pressure or p-mode pulsations typically have periods of a few minutes; gravity or g-modes have periods of the order of an hour. See, for example, Heber (2016).

\* E-mail: sumanta.kumar27@gmail.com

Data are downloaded and processed in the same way as explained in Papers I and II. For a convenient comparison, the Tables presented here will preserve the listing order from the previous papers of this series, however some of the tables from Paper I are merged to be consistent with those in Paper II. They also contain the most important information from Papers I and II with additional information resulting from this work. In the following sections, we explain the details of the contamination analysis and provide the results of this work.

## 2 CONTAMINATION ANALYSIS

We defined each target mask as a square of  $11 \times 11$  pixels, which provides enough pixels to clarify contamination, if any. We used our custom PYTHON scripts to retrieve fluxes separately from each pixel in a  $3 \times 3$  pixel square centered at a given target. Then, for each of the nine pixels, we calculated an amplitude spectrum and checked if the signals reported in Papers I and II is detected in pixels that overlap with the location of the target. We employed either PanSTARRS or DSS images and overlapped them with target pixel files (TPF) created from the TESSCUT tool (Brasseur et al. 2019). In specific cases, that is, bright stars in target masks, even though far enough from our targets not to contaminate them, we calculated the amplitude spectra in pixels covering these stars to check for their variability. As a result of our contamination analysis, we derived a few common cases, listed below (the columns refer to Tables in the online materials):

- A signal comes only from the target star, which means no contamination and the target listed in Papers I and II is the source of the variability (Figure 1). In the VARIABLE CONTAMINATOR column of Tables 1-14, we marked these cases with *none*.
- A signal comes from a contaminating object (Figure 2). These cases have the name of the contaminator listed in the VARIABLE CONTAMINATOR column. In parentheses, we added additional information on the contaminators collected from the SIMBAD database. If these contaminators are new variable stars, then they are also listed in Table 16. This is a false positive case.
- A signal comes from both the target and contaminating object(s) (Figure 3). These cases will have frequencies assigned to either our target (marked as *none*) or contaminator(s) listed in the VARIABLE CONTAMINATOR column. This is the case of a variable target showing an additional signal, which is a false positive.
- No signal is detected in single pixels (Figure 4). These cases are caused by low S/N in merged pixels defined in Papers I and II. In the VARIABLE CONTAMINATOR column we marked these cases with *no signal in individual pixels*. This case is not verified, however remarks on nearby stars listed in tables in Papers I and II give some clue on the possible contamination.
- A signal is detected in all pixels across a target mask (Figure 5). In the VARIABLE CONTAMINATOR column we marked these cases with *signal in all pixels*. This is a false positive case. The source of the signal is either a nearby bright object that shines over a large area or an instrumental artifact.
- A nearby non-contaminating bright object (within the target mask) has been verified positively for its variability (Figure 6). These new variable stars are listed in Table 16.

The full tables with remarks of our contamination analysis are presented in the online materials. The most interesting conclusions of our contamination analysis are the following:

- Among two sdBV candidates from Paper I, TIC 237597052, is

no longer considered a candidate. It turned out to be a main sequence B8 star (Table 1). Our fit to a spectrum which we collected from the LAMOST survey provides the following atmospheric parameters,  $T_{\text{eff}} = 12460(300)$  K,  $\log(g/\text{cm s}^{-2}) = 4.17(12)$ . The other candidate is a confirmed sdB star, so TIC 262753627 is a new sdB pulsator.

- Out of 13 sdBV candidates listed in Paper II, five are no longer considered the sources of the signal. Apart from these five contaminated targets, TIC 363766470 is also partially contaminated by ATO J265.8117+21.5538. However, our target is still the source of the  $116.44 \mu\text{Hz}$  frequency. The contamination of one case could not be verified, while the remaining seven sdBs including TIC 363766470 are confirmed pulsators. ATO J265.8117+21.5538 is listed in the SIMBAD database as an eclipsing binary candidate and we confirm this type by detecting signal at a frequency of  $41.09 \mu\text{Hz}$  along with its harmonics. We determined an orbital period of 0.28169 days (Table 2).

- Among 66 other (than the above) variable sdBs listed in Papers I and II, we found 14 not to be the sources of the variable signals. Six cases are not verified. The remaining 46 are confirmed variable sdBs (Tables 1 and 2).

- Out of 10 sdV candidates listed in Paper II, four are no longer considered to be the sources of the signals, while TIC 194781979 was identified as a main sequence B6 star. One case is not verified. The remaining four sdVs are confirmed pulsating candidates (Table 3).

- Among 23 other (than the above) variable sdVs listed in Paper II, we found seven targets not to be the sources of the signal. Four cases are not verified. The remaining 12 sdVs are confirmed variables (Table 3).

- Among 113 spectroscopically unclassified pulsators, we found 68 targets not to be the sources of the signal. Seven cases are not confirmed. The remaining 38 original targets are confirmed pulsators. In the case of TIC 311792028, the  $95.37 \mu\text{Hz}$  frequency along with its harmonics are native to TIC 311792021, while the  $34.14 \mu\text{Hz}$  frequency originating in our target does not seem to be related to pulsations (Tables 4 and 5).

- Among 106 candidate eclipsing binaries, we found 65 targets not to be the sources of the signal. We do not confirm the variability of TIC 847473488. We found 38 original targets to be confirmed eclipsing binaries. In the case of TIC 1509561926, the eclipses originate in TYC 9289-2657-1, while our target itself shows only the  $102.89 \mu\text{Hz}$  frequency. In the case of TIC 159448831, the target is contaminated by an eclipsing binary TIC 159448824, however our target shows  $158.68 \mu\text{Hz}$  along with harmonics. These frequencies, though, are not responsible for the eclipses we plot in Figure 9 in Paper II (Tables 6 and 7).

- Among 248 binaries showing one symmetric maximum, we found 118 targets not to be the sources of the signal. Five cases are not verified. We found 125 original targets that are confirmed variables. TIC 377658867 shows a significant signal at  $54.28 \mu\text{Hz}$  and its harmonics, though the contaminator TIC 378037013 shows  $76.27 \mu\text{Hz}$  frequency. Likewise in TIC 388622589, which shows  $13.77 \mu\text{Hz}$  frequency, while a contaminator TIC 388622573 is responsible for the  $161.92 \mu\text{Hz}$  frequency. On the other hand, TIC 463006021 is heavily contaminated by two sources, even though the target still shows  $53.01 \mu\text{Hz}$  frequency and its harmonics. TIC 463006006 shows the  $9.03 \mu\text{Hz}$  frequency presented in Paper I, while TIC 463006054 shows a  $6.71 \mu\text{Hz}$  frequency and its harmonics. In the case of TIC 2040326958, it is actually TIC 10596964 that shows the  $7.87 \mu\text{Hz}$  frequency and its harmonics reported in

**Table 1.** Southern Ecliptic Hemisphere (SEH) – 28 objects classified as *sdBs*. Only the first five objects are listed while the full table can be found in the online materials.

No.	<i>Gaia</i> DR2	TIC	Name	G [mag]	Period [d]	Variable contaminator
<i>sdBVs</i>						
1	3129751228471383808	237597052	TYC 161-49-1	11.14	0.05-0.1	none
2	3159937564294110080	262753627	TYC 770-941-1	12.46	0.04-0.08	none
Phased lightcurves						
1	2333936291513550336	12379252	Ton S138	16.01	0.2648	none
2	2385348183917624448	9035375	PHL 460	12.21	0.4734	none
3	296943820688996160	139397815	-	13.61	0.2746	none

**Table 2.** Northern Ecliptic Hemisphere (NEH) – 53 objects classified as *sdBs*. Only the first five objects are listed while the full table can be found in the online materials.

No.	<i>Gaia</i> DR2	TIC	Name	G [mag]	Period [d]	Variable contaminator
<i>sdBVs</i>						
1	1028374599849118976	802232206	SDSSJ082428.41+512601.6	18.72	0.1734	CRTS J082433.5+512441 (EB)
2	127674641678296704	353892824	KUV02281+2730	15.15	0.0487	none
3	1345049483546987904	159850392	GALEXJ17566+4125	14.28	0.08 - 0.13	none
4	1469357759922416256	321423000	SDSSJ132432.37+320420.9	16.64	0.0907	TIC 321422994
5	1495329392800826624	23746001	PG1350+372	14.31	0.06 - 0.09	none

**Table 3.** NEH – 33 objects classified as *sds*. Only the first five objects are listed while the full table can be found in the online materials.

No.	<i>Gaia</i> DR2	TIC	Name	G [mag]	Period [d]	Variable contaminator
<i>sdVs</i>						
1	1906485375099435136	259091223	FBS2209+354	14.30	0.07-0.13	no signal in individual pixels
2	1952553606634620928	407657360	LAMOSTJ214600.31+372119.7	14.66	0.045 - 0.1	TIC 407657373
3	2041883531914920064	20688004	GALEXJ18578+3048	13.73	0.1726	ATO J284.4865+30.8044 (EB candidate)
4	2128012018629286144	1882679963	KeplerJ19352+4555	17.16	0.1766	ATO J293.8168+45.8972 (EB candidate)
5	237650985848157312	194781979	LAMOSTJ032717.71+410344.5	10.19	0.1594	none

Paper II, though our target still shows a  $131.94 \mu\text{Hz}$  frequency (Tables 8 and 9).

- Among 52 binaries showing one asymmetric maximum, we found 42 targets not to be the sources of the signal. The remaining 10 original targets are confirmed variables. TIC 79689537, which shows a  $82.64 \mu\text{Hz}$  frequency and its harmonics, is heavily contaminated by two objects. TIC 79689505 shows the  $3.7 \mu\text{Hz}$  frequency and its harmonics reported in Paper I, while ATO J104.6541-23.0081 shows a  $5.56 \mu\text{Hz}$  frequency and its harmonics (Tables 8 and 9).

- Among 66 binaries showing two maxima, we found 49 targets not to be the source of the signal. The remaining 17 targets are confirmed binaries (Tables 8 and 9).

- The two novae listed in Paper I are not contaminated (Table 10).

- Among 1490 spectroscopically unclassified targets showing signal in their amplitude spectra, we found 719 not to be the sources of the signal while 460 cases are not verified. Such a high number of these cases is a consequence of a low signal that is not detectable in individual pixels. The remaining 311 original targets are confirmed variables. In five cases, our original targets show a signal, although it may not be the one reported in Papers I or II (Tables 11 and 12).

- Among 122 spectroscopically classified non-*sdB* stars, we found 14 targets not to be the sources of the signal. Nine cases are not verified, while the remaining 99 original targets are confirmed variables (Tables 13 and 14).

To summarize our contamination analysis, we found 1141 targets not to be the sources of the signal, while 451 targets were not

verified. This leaves us with 721 variable *sdB* candidates remaining, including both pulsating and binary stars.

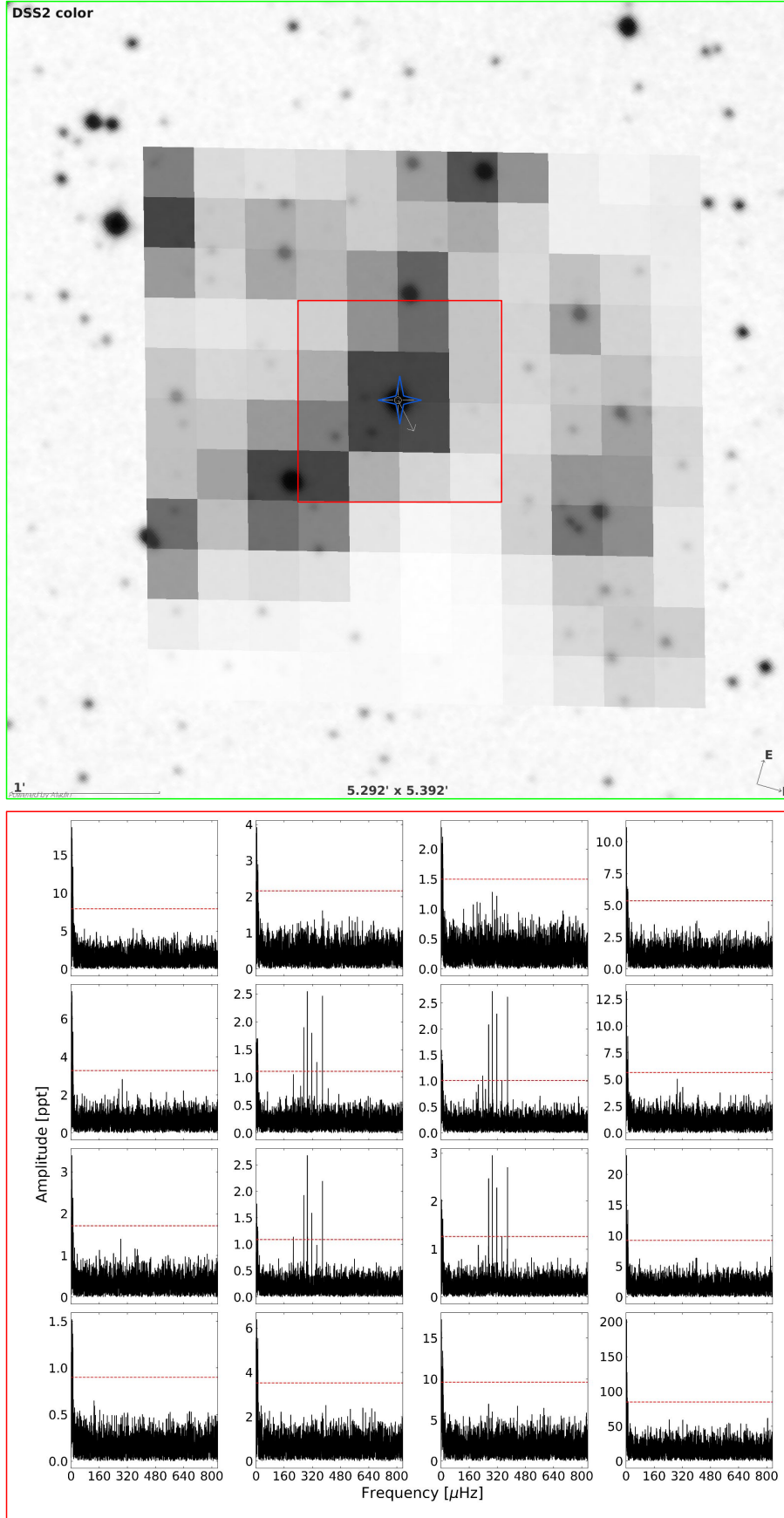


**Figure 1.** Contamination analysis for TIC 323174439, representing an uncontaminated object. Top panel: target mask overlapped with a DSS2 image. The blue star indicates the target. The red box defines the pixels for which the amplitude spectra were calculated. Bottom panel: Amplitude spectra of the 16 pixels within the red box in the top panel.

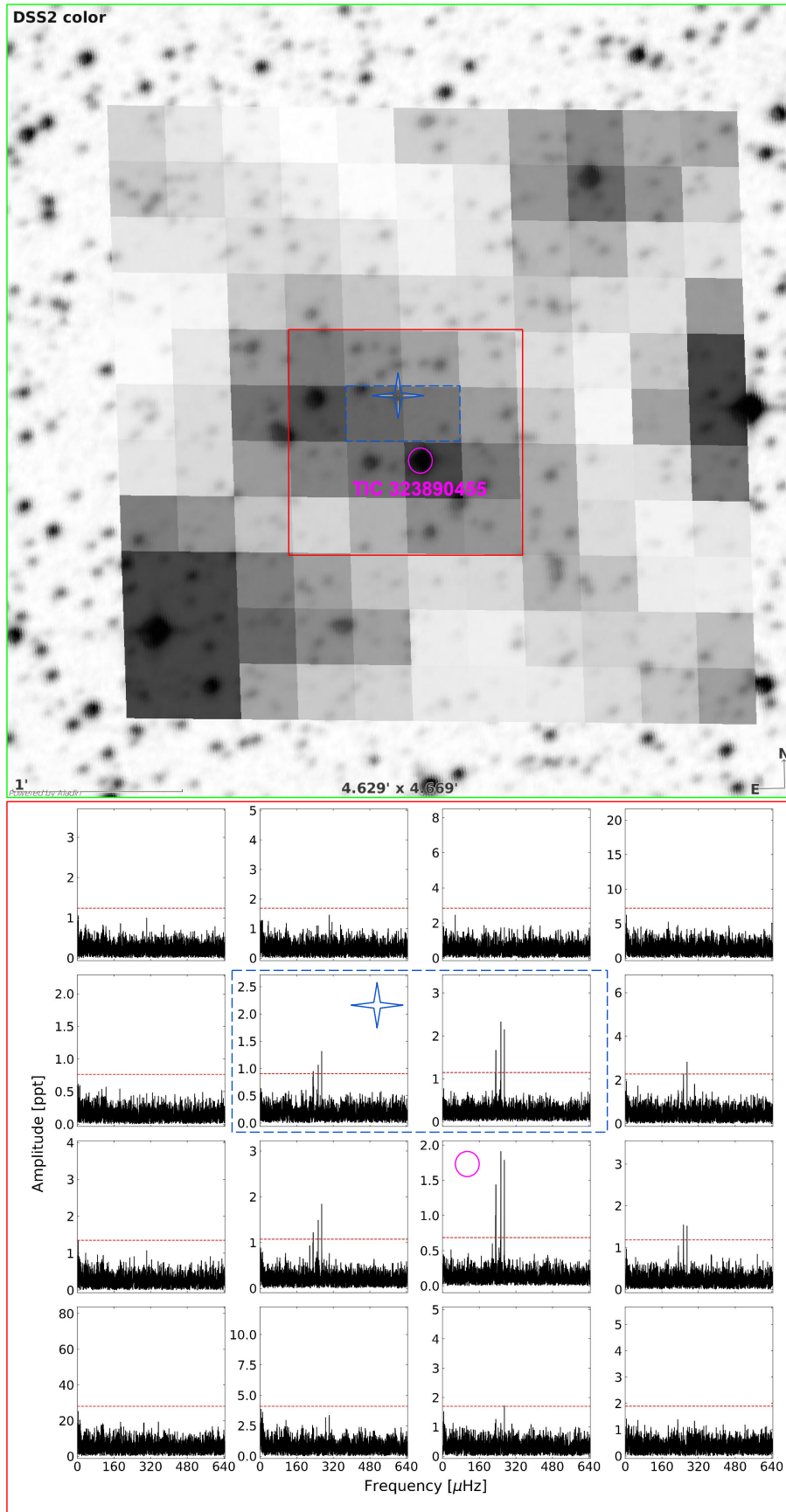


**Figure 2.** Contamination analysis for TIC 1514267365, representing a false positive case. The marks and colors are the same as in Figure 1. The blue rectangle represents the aperture used in Paper I. The dominant signal comes from pixels centered on TIC 323890455 (magenta circle in the top panel) and overlaps with the aperture used in Paper I.

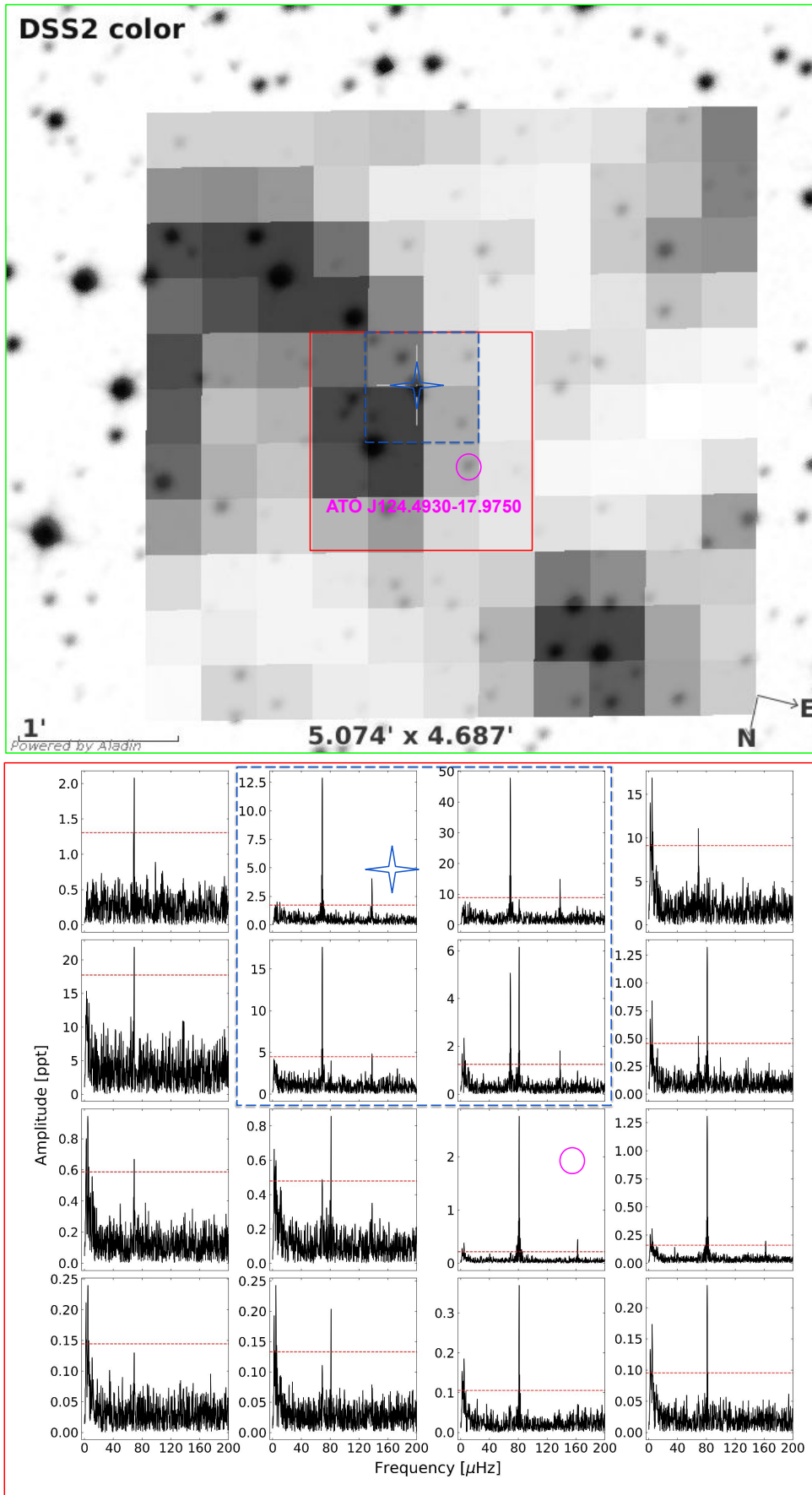


**Figure 3.** Contamination analysis for TIC 218791808, representing the signal coming from both the target and a neighboring object. The marks and colors are the same as in Figure 1. The blue dashed box represents the aperture used in Paper I.

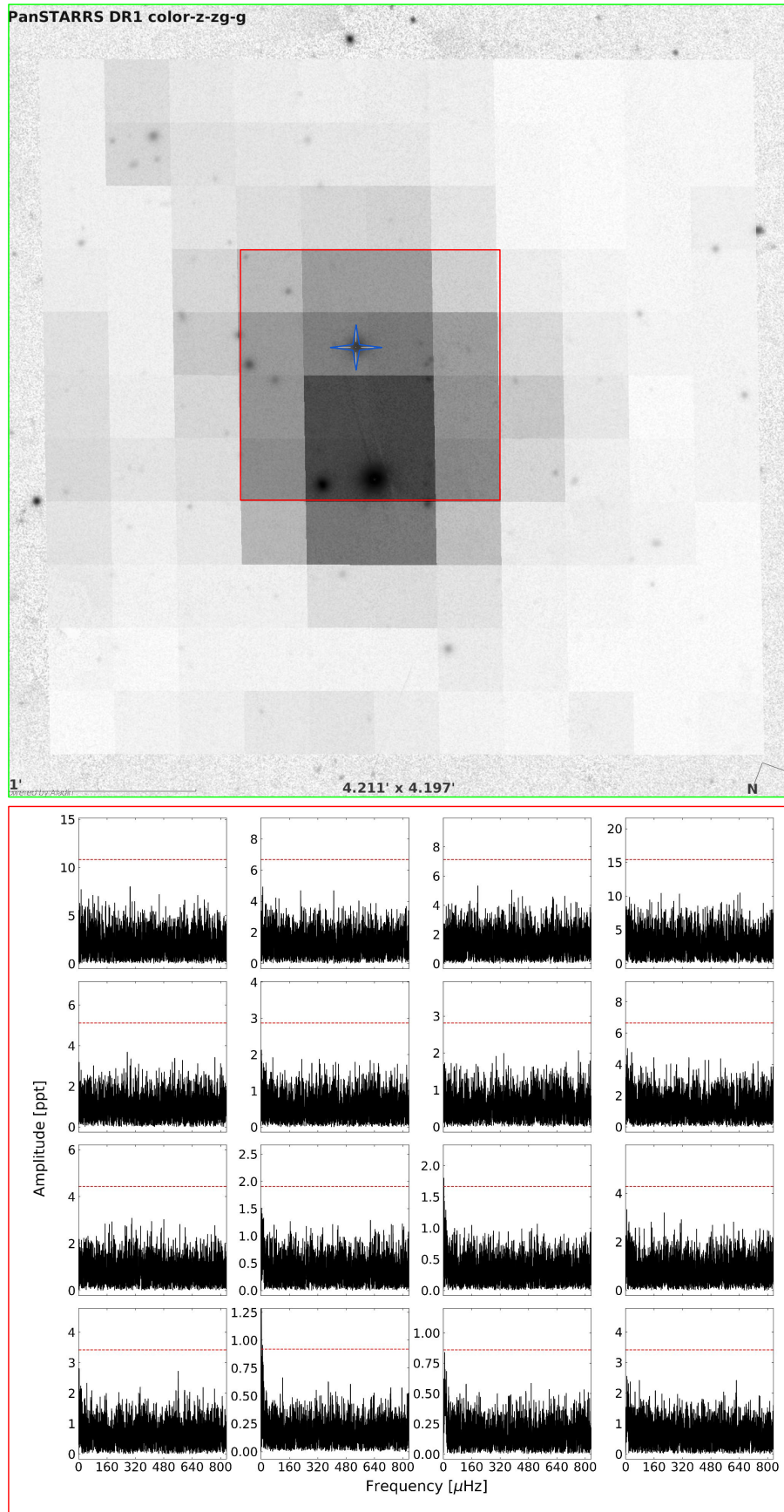


**Figure 4.** Contamination analysis for TIC 275358553, representing an unconfirmed case. The marks and colors are the same as in Figure 1 but a PanSTARRS DR1 image is used instead. No significant signal is detected in any of the individual pixels.

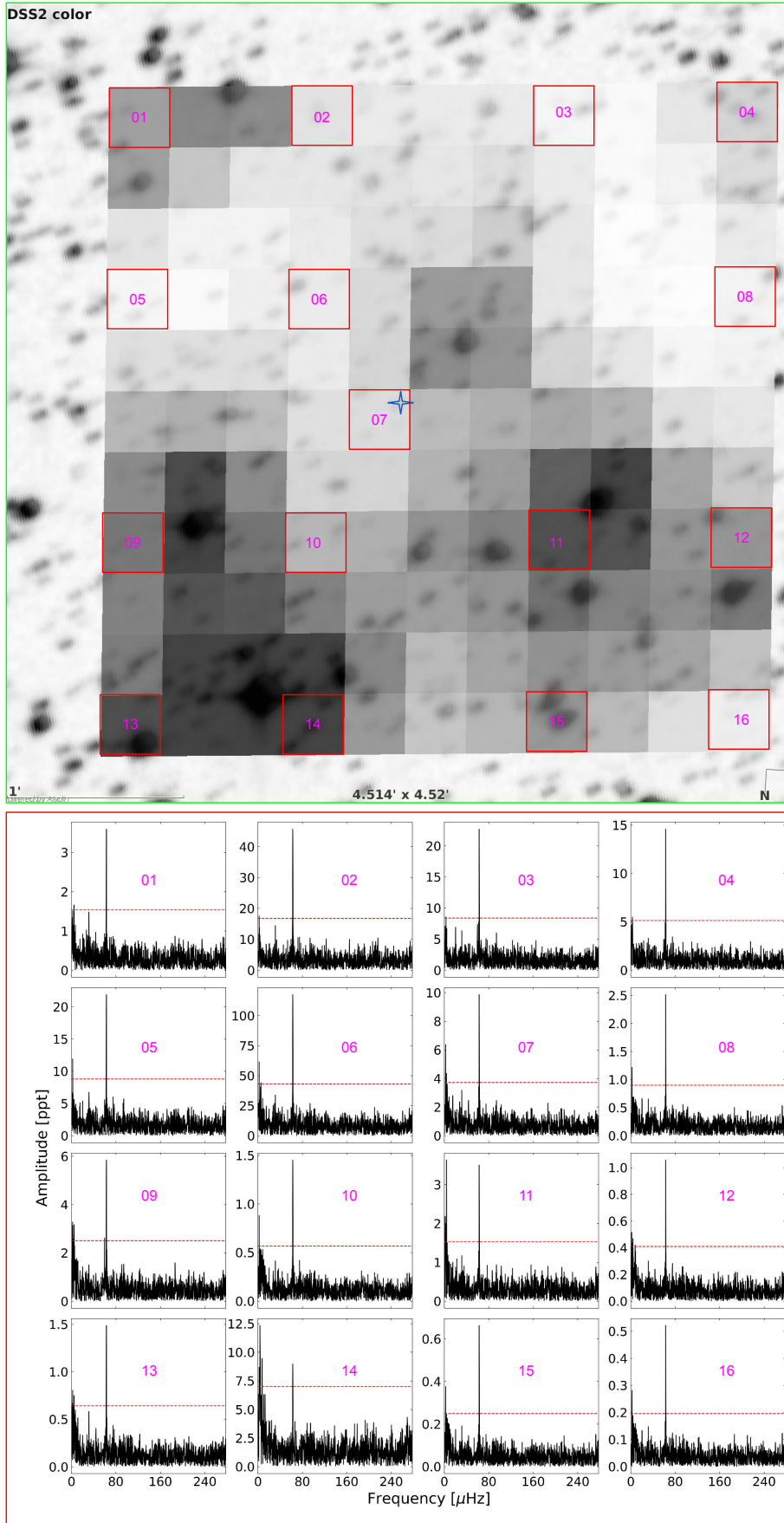


**Figure 5.** Contamination analysis for TIC 1314011445, representing a false positive case. The marks and colors are the same as in Figure 1. Magenta numbers in selected pixels correspond to amplitude spectra shown in the bottom panel. The location of the source of the signal is unconstrained.



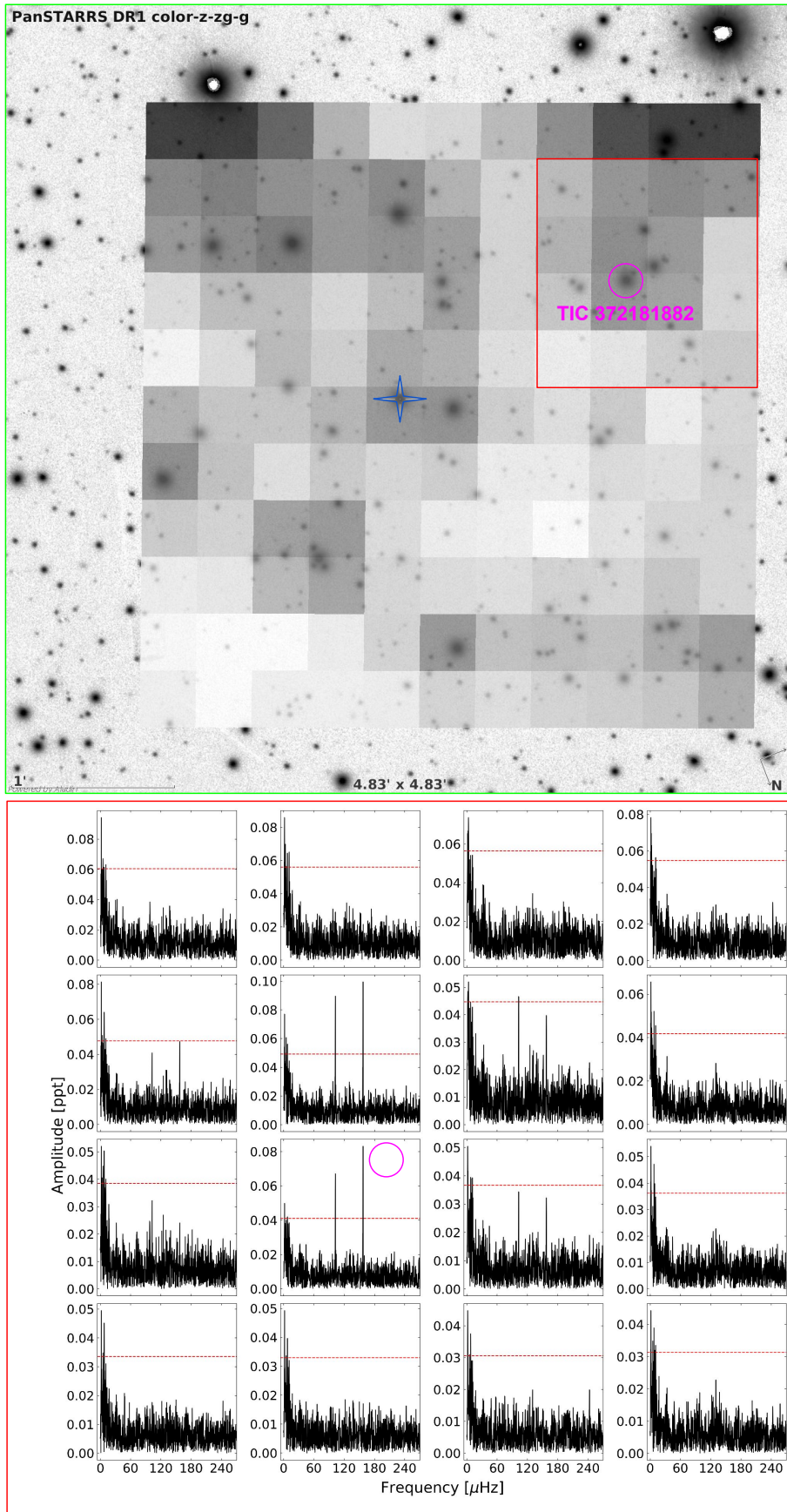


**Figure 6.** Contamination analysis for TIC 372181885 (the blue star mark). It is an example of discovering a new non-contaminating variable star (magenta circle) within the target mask during the contamination check of target of interest. The marks and colors are the same as in Figure 2.

**Table 4.** SEH – 83 pulsator candidates. Only the first five objects are listed while the full table can be found in the online materials.

No.	<i>Gaia</i> DR2	TIC	G [mag]	Variable contaminator
1	2921500461998485248	744231977	18.31	TYC 6526-2198-1
2	2927637764107094272	744958933	18.67	ATO J106.3086-23.5750
3	3062196993541803904	754827446	17.45	TYC 4817-751-1
4	3087146252404755584	257068255	15.08	none
5	3111790534231122944	284329074	15.26	TYC 163-370-1

**Table 5.** NEH – 30 pulsator candidates. Only the first five objects are listed while the full table can be found in the online materials.

No.	<i>Gaia</i> DR2	TIC	G [mag]	Variable contaminator
1	1422182595056481536	320525680	13.87	no signal in individual pixels
2	1943952161530528256	431548978	15.61	no signal in individual pixels
3	1974973679520560896	311792028	15.88	34.14 $\mu$ Hz: none; 95.37 $\mu$ Hz+harmonics: TYC 3605-1317-1 (V)
4	1988552407605096320	66784300	14.88	TIC 66784249
5	1991879937806406656	2044241813	18.47	NSVS 1502401 (EB)

**Table 6.** SEH – 83 eclipsing binaries. Only the first five objects are listed while the full table can be found in the online materials.

No.	<i>Gaia</i> DR2	TIC	G [mag]	Period [d]	Variable contaminator
32 eclipsing binaries that show both primary and secondary eclipses					
1	2938186341221700480	60523137	16.23	1.2532	none
2	3056677303432024960	753916356	17.97	2.4282	TIC 68060528
3	4037952609036313728	1556986400	18.86	4.2844	TIC 368875977
4	4038037855601783296	1557298522	17.18	2.9735	TYC 7404-5579-1
5	4044609357370901632	1569961982	16.46	2.415	RS Sgr (B3/4IV/V, EB)

**Table 7.** NEH – 23 eclipsing binaries. Only the first five objects are listed while the full table can be found in the online materials.

No.	<i>Gaia</i> DR2	TIC	G [mag]	Period [d]	Variable contaminator
Eclipsing binaries that show only primary eclipses					
1	1131845039229607680	459182998	16.16	0.2344	49.77 $\mu$ Hz+harmonics: none; 6.94 $\mu$ Hz+harmonic: TIC 459183003
2	1417117518648285056	1400704733	17.03	0.3637	none
3	1816806183083980288	1943324398	17.22	1.3135	HD 195052 (F8)
4	1840900601716813440	1951174238	18.92	1.0329	TIC 126684646
5	1846629538332584960	15040115	11.83	0.8099	none

**Table 8.** SEH – 273 spectroscopically unclassified variables with phased light curves. Only the first five objects are listed while the full table can be found in the online materials.

No.	<i>Gaia</i> DR2	TIC	G [mag]	Period [d]	Variable contaminator
One symmetric maximum					
1	2896588449084891136	49547169	13.28	0.3086	IS CMa (F3V)
2	2905822663130146688	31353391	14.03	0.8929	none
3	2909497952544966272	37118148	14.28	0.2681	none
4	2911497105202950400	37004041	15.16	0.2833	none
5	2921050693020996864	63113578	11.45	0.4854	none

**Table 9.** NEH – 93 spectroscopically unclassified variables with phased light curves. Only the first five objects are listed while the full table can be found in the online materials.

No.	<i>Gaia</i> DR2	TIC	G [mag]	Period [d]	Variable contaminator
One symmetric maximum					
1	1000519267329142144	444946935	15.92	1.6725	none
2	1086341235118052096	85158691	12.85	0.3546	none
3	1099487030500185344	743328948	16.90	0.3297	none
4	1133795950814826240	841399917	17.31	1.5134	none
5	1141625057721183616	138400883	16.24	0.0680	none

**Table 10.** SEH – two novae. This table is also included in the online materials.

No.	<i>Gaia</i> DR2	TIC	Name	G [mag]	Variable contaminator
1	5207384891323130368	735128403	AH Men	13.51	none
2	6544371342567818496	121422158	RZ Gru	12.63	none

**Table 11.** SEH – 1262 spectroscopically unclassified variables with amplitude spectra. Only the first five objects are listed while the full table can be found in the online materials.

No.	<i>Gaia</i> DR2	TIC	G [mag]	Variable contaminator
1	2326333512204996992	380826878	15.69	none
2	2342907791000463232	610076106	17.18	[SHM2017] J013.19449-26.56892 (RR Lyr)
3	2342907962798690944	610077229	16.68	[SHM2017] J013.19449-26.56892 (RR Lyr)
4	2409630520260038784	2052262357	18.09	CI* NGC 7492 C 1306 (RR Lyr)
5	2410677839445234944	111183765	14.48	none

**Table 12.** NEH – 228 spectroscopically unclassified variables with amplitude spectra. Only the first five objects are listed while the full table can be found in the online materials.

No.	<i>Gaia</i> DR2	TIC	G [mag]	Variable contaminator
1	1082306439760979840	743148169	18.81	TIC 284473271
2	1107705772542003200	705157619	18.09	no signal in individual pixels
3	1108642968765677696	743476657	18.74	V486 Cam (RR Lyr)
4	1112770367915047424	705166070	17.41	none
5	1113516073020001152	705175423	18.32	TIC 468921975

**Table 13.** SEH – 76 non-sdB classified variables. Only the first five objects are listed while the full table can be found in the online materials.

No.	<i>Gaia</i> DR2	TIC	G [mag]	spT	Period [d]	Variable contaminator
Pulsators						
1	2969201399574096128	708596809	11.30	A0IV/V	-	no signal in individual pixels
2	3109409266919646976	168595004	10.70	A5	-	none
3	3115125211261708032	293137161	11.01	A0	-	none
4	3344114626761364224	437889214	10.02	B5	-	none
5	3396397877830881792	247513086	8.17	A0	-	none

**Table 14.** NEH – 46 non-sdB classified variables. Only the first five objects are listed while the full table can be found in the online materials.

No.	<i>Gaia</i> DR2	TIC	G [mag]	spT	Period [d]	Variable contaminator
Pulsators						
1	1625627602365544832	198209459	13.53	B2	-	none
2	1713032695100155904	298091568	15.00	B4.1	-	none
3	1861191062326013696	1955410399	10.31	A0	-	none
4	2077737678383889408	270610177	11.77	Be	-	11 $\mu$ Hz+harmonics: none; 46 - 70 $\mu$ Hz: UCAC4 663-077912 (PuIV)
5	2132171608553758336	279919275	13.46	B3V	-	none

### 3 UPDATED AMPLITUDE SPECTRA AND NEW PULSATING SDB STARS

We took advantage of access to the 10 min FFI data collected during Years 3 and 4 to discover new variable sdB stars and to improve the amplitude spectra for known sdBV stars. Not all variable stars listed in Papers I and II were subject to this updated analysis. Binaries would surely benefit from a three times better sampling, which would yield much better definition of eclipses and more precise orbital period estimation, but it would not affect their variability type. The contaminated stars, which turned out not to be sources of the signal, were also excluded. We focused only on targets that show rich signal close to the  $277.7 \mu\text{Hz}$  Nyquist frequency, which appear to be quite convincing pulsations. In these cases shifting the Nyquist frequency to a three times higher value would uncover the entire g-mode region of possible pulsating sdB stars. We ended up with a final list of 78 targets.

The light curve extraction process and data reduction of the 10 min FFI data, are the same as for the 30 min FFI data described in Papers I and II, where we refer the reader for details. Out of 78 pre-selected targets we found 24 that show multiple frequencies, which we interpret as pulsations, and the number of frequencies were significantly increased or more frequencies beyond the  $277.7 \mu\text{Hz}$  Nyquist frequency were detected. We list these targets in Table 15 in the online material. The targets are confirmed as the original sources of the detected signals. We show the amplitude spectra of these 24 targets in Figure 7. We marked the typical g-mode frequency range (*i.e.*  $100\text{--}400 \mu\text{Hz}$ ) with dashed vertical lines. This region overlaps with the typical p-mode frequency range of  $\delta$  Scuti stars, so it is not generally straightforward to claim the detection of a pulsating sdB star based only on the amplitude spectrum content. Alternatively, if the frequencies detected are outside the indicated

range, we might well doubt the detection of an sdB pulsator. For instance, TIC 224284872 is an A star and the frequencies are outside the expected range. Similarly, TIC 181142865 turned out to be a main sequence star. TIC 437889214 shows frequencies below the expected region – its spectral type is B5. There are other targets which are not classified as hot subdwarfs, yet show frequencies in the range characteristic of pulsating sdB stars. These cases may be either  $\delta$  Scuti pulsators or misclassified hot subdwarfs. We confirm a detection of g-mode pulsations in 11 sdB pulsators. TIC 442750342 seems to be an exception in our sample being a low gravity and cool sdB pulsator.

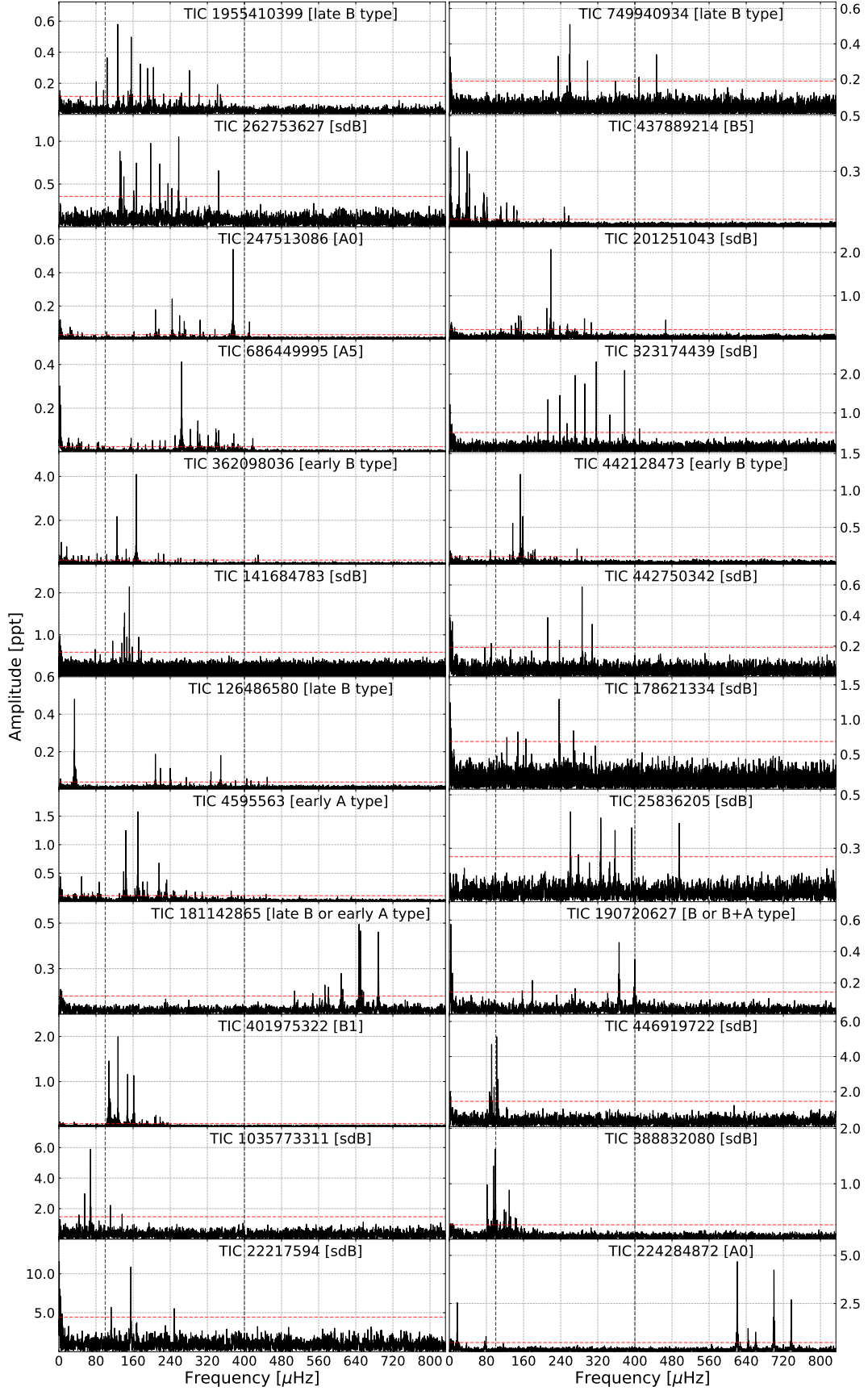


**Figure 7.** The amplitude spectra of pulsators analyzed with 10 min FFI data. Vertical dashed lines indicate the typical g-mode region of pulsating hot subdwarfs. The horizontal lines mark the detection thresholds.

**Table 15.** Pulsators confirmed with the 10 min FFI data. We show amplitude spectra of these objects in Figure 7. This table is also included in the on-line materials.

No.	<i>Gaia</i> DR2	TIC	G [mag]	Variable contaminator	Remarks
1	1861191062326013696	1955410399	10.66	none	late B type
2	3032890473180888192	749940934	12.46	none	late B type
3	3159937564294110080	262753627	12.46	none	sdB
4	3344114626761364224	437889214	10.16	none	B5
5	3396397877830881792	247513086	8.44	none	A0
6	4923853724788504192	201251043	11.93	none	sdB
7	5090382015016433920	686449995	6.99	none	A5
8	5196271513123121152	323174439	13.30	none	sdB
9	5250674622612902912	362098036	11.48	none	early B type
10	5257747299878049152	442128473	10.84	none	early B type
11	5266133451162548864	141684783	14.53	none	sdB
12	5307946881949072000	442750342	12.82	none	sdB
13	5326745919424790656	126486580	9.30	none	late B type
14	5362558250096941056	178621334	13.33	none	sdB
15	5429254969036524416	4595563	10.11	none	early A type
16	5439887654492064256	25836205	13.14	none	sdB
17	5525342630213336448	181142865	11.11	none	late B or early A type
18	5622554881336253824	190720627	11.07	none	B or B+A type
19	5796399012705196800	401975322	10.21	none	B1
20	5823403087017696384	446919722	12.96	none	sdB
21	5872410931625754624	1035773311	17.46	none	sdB
22	5922070855307705472	388832080	12.58	none	sdB
23	6143764182206682112	22217594	15.16	none	sdB
24	6534581776366266752	224284872	13.53	none	A0

#### 4 NEW VARIABLES

As a by-product of the contamination analysis we report the true sources of variability preliminarily assigned to the targets listed in Papers I and II. In Tables 1-14 we provide a `VARIABLE CONTAMINATOR` column which, in the case of a positive variability contamination, contains a name of a contaminator. In addition, we detected new variables that do not contaminate our pre-selected targets but are located within the target masks of our targets. For a practical reason, all these variable contaminators and new non-contaminating variables are listed in Table 16 in the online materials. In total, we report detection of 682 new variable stars, including two, listed last in Table 16, that have no *Gaia* (Gaia Collaboration et al. 2018) designation yet. To be precise, the discovery of the variability of the majority of these stars was presented in Papers I and II, so only 97 stars are found to be new variables (accounting for Papers I and II) while the remaining 585 stars now have the variability properly assigned (as compared to Paper I and II).

**Table 16.** Basic information of the 682 new variable stars found during the contamination analysis in both SEH and NEH. Only first five objects are listed while the full table can be found in the online materials.

No.	<i>Gaia</i> DR2	TIC	Name	G [mag]
1	1000847845211000960	14196021	-	16.65
2	1030011910101662336	467154863	-	12.56
3	1082306439760980224	284473271	-	16.95
4	1113516077316307328	468921975	-	17.32
5	1131845245388039296	459183003	-	14.38

## 5 SUMMARY

We presented the results of our contamination analysis of stars included in Papers I and II. We identified 1 141 false positives, while 451 variables were not verified because, in most cases, the signal is of too low amplitude to be detected in individual pixels. The total number of targets, which are the sources of the signal we presented in Papers I and II is 721. As a by-product of our contamination analysis we found 97 new variables that happened to be within target masks of our original stars listed in Papers I and II. In total, we analysed 2 995 targets in TESS fields, where 2313 targets were presented in Papers I and II and the remaining 682 variable targets were found during the contamination check. Out of the 2 313 targets, we confirmed 721 as variable after contamination analysis. Hence the total number of variable targets we found is 1 403.

We pre-selected 78 uncontaminated targets that are pulsator candidates (that is, they show rich pulsation content close to the 277.7  $\mu$ Hz Nyquist frequency) for additional analysis using the 10 min FFI data collected during Years 3 and 4. We ended up with 24 targets for which those new data turned out to be beneficial – that is, more peaks either below, or especially beyond, the 277.7  $\mu$ Hz frequency were detected. For any of these 24 stars without spectral type, we used publicly available data and/or spectroscopic data collected with the 1.9 m telescope at the South African Astronomical Observatory to identify hot subdwarfs. In total, we found 11 new sdB pulsators. Details of the spectroscopic analysis will be provided in Worters et al. (in preparation).

One of the pulsator candidates, TIC 362098036, was a subject of a pulsation mode identification and the result was reported in Paper I. Our analysis confirmed that the target is a main sequence B star, which makes the mode identification irrelevant.

## ACKNOWLEDGEMENTS

Financial support from the National Science Center in Poland under projects No. UMO-2017/26/E/ST9/00703 and UMO-2017/25/B/ST9/02218 is acknowledged. PN acknowledges support from the Grant Agency of the Czech Republic (GAČR 22-34467S). The Astronomical Institute in Ondřejov is supported by the project RVO:67985815. This paper includes data collected by the *TESS* mission. Funding for the *TESS* mission is provided by the NASA Explorer Program. This work has made use of data from the European Space Agency (ESA) mission *Gaia* (<https://www.cosmos.esa.int/gaia>), processed by the *Gaia* Data Processing and Analysis Consortium (DPAC, <https://www.cosmos.esa.int/web/gaia/dpac/consortium>). Funding for the DPAC has been provided by national institutions, in particular, the institutions participating in the *Gaia* multilateral agreement. This research has used the services of [www.Astroserver.org](http://www.Astroserver.org).

## DATA AVAILABILITY

The datasets were derived from MAST in the public domain archive.stsci.edu.

## REFERENCES

- Baran A. S., Sahoo S. K., Sanjayan S., Ostrowski J., 2021, *Monthly Notices of the Royal Astronomical Society*, 503, 3828
- Brasseur C. E., Phillip C., Fleming S. W., Mullally S. E., White R. L., 2019, *Astrocut: Tools for creating cutouts of TESS images* (ascl:1905.007)
- Gaia* Collaboration et al., 2018, *A&A*, 616, A1
- Geier S., 2020, *A&A*, 635, A193
- Geier S., Raddi R., Gentile Fusillo N. P., Marsh T. R., 2019, *A&A*, 621, A38
- Heber U., 2016, *PASP*, 128, 2001
- Sahoo S. K., Baran A. S., Sanjayan S., Ostrowski J., 2020, *Monthly Notices of the Royal Astronomical Society*, 499, 5508

This paper has been typeset from a  $\text{\TeX}/\text{\LaTeX}$  file prepared by the author.